

Observation of time-invariant coherence in a room temperature quantum simulator

Isabela A. Silva,^{1,2} Alexandre M. Souza,³ Thomas R. Bromley,² Marco Cianciaruso,^{2,4,5} Roberto S. Sarthour,³ Ivan S. Oliveira,³ Rosario Lo Franco,^{1,2,6} Eduardo R. deAzevedo,¹ Diogo O. Soares-Pinto,¹ and Gerardo Adesso^{2*}

¹*Instituto de Física de São Carlos, Universidade de São Paulo, CP 369, 13560-970, São Carlos, SP, Brazil*

²*School of Mathematical Sciences, The University of Nottingham, University Park, Nottingham NG7 2RD, United Kingdom*

³*Centro Brasileiro de Pesquisas Físicas, Rua Dr. Xavier Sigaud 150, 22290-180 Rio de Janeiro, RJ, Brazil*

⁴*Dipartimento di Fisica “E. R. Caianiello”, Università degli Studi di Salerno, Via Giovanni Paolo II, I-84084 Fisciano (SA), Italy*

⁵*INFN, Sezione di Napoli, Gruppo Collegato di Salerno, I-84084 Fisciano (SA), Italy*

⁶*Dipartimento di Energia, Ingegneria dell’Informazione e Modelli Matematici (DEIM),
Università di Palermo, Viale delle Scienze, Ed. 9, I-90128 Palermo, Italy*

*To whom correspondence should be addressed; E-mail: gerardo.adesso@nottingham.ac.uk

(Dated: November 5, 2015)

The ability to live in coherent superposition states is a signature trait of quantum systems and constitutes an unexpendable resource for quantum-enhanced technologies. However, decoherence effects usually destroy quantum superpositions. Here we show that, in a composite quantum system exposed to decohering noise, quantum coherence in a reference basis can stay protected for indefinite time. This occurs for a class of quantum states independently of the measure used to quantify coherence, and requires no control on the system during the dynamics. Such an invariant coherence phenomenon is observed experimentally in a two-qubit room temperature nuclear magnetic resonance quantum simulator. Our study reveals a novel interplay between coherence and various forms of correlations, and highlights the natural resilience of quantum effects in complex systems.

Successfully harnessing genuine nonclassical effects is predicted to herald a new wave of technological devices with a disruptive potential to supersede their conventional counterparts [1]. Such a prediction is now coming of age and conspicuous international engagements are being devoted to translating the astounding power of quantum technologies into concrete applications for sectors as diverse as networked communication, computing, imaging, sensing and simulation [2]. Quantum coherence, which incarnates the wavelike nature of matter and the essence of quantum parallelism [3], is the primary ingredient enabling a supraclassical performance in a wide range of such applications. Its key role in optics, metrology, condensed matter physics and nanoscale thermodynamics is actively investigated and widely recognised [4–6]. Furthermore, coherent quantum effects have been observed in large molecules [7] and are advocated to play a functional role in even larger biological complexes [8–11]. However, coherence is an intrinsically fragile property which typically vanishes at macroscopic scales of space, time, and temperature: the disappearance of coherence, commonly referred to as decoherence [12], in quantum systems exposed to environmental noise is one of the major hindrances still threatening the scalability of most quantum machines. Numerous efforts have been thus invested in recent years into devising feasible control schemes to preserve coherence in open quantum systems, with notable examples including dynamical decoupling [13, 14], quantum feedback control [15] and error correcting codes [16].

In this paper we demonstrate a fundamentally different mechanism. We show that quantum coherence in a composite system, whose subsystems are all affected by decoherence, can remain invariant for unlimited time without any external control. This phenomenon was recently predicted to occur for a particular family of initial states of quantum systems of many qubits [17], and is here observed in a two-qubit spin ensemble realised by a room temperature liquid-state nuclear

magnetic resonance (NMR) quantum simulator [18–20]. After the initialisation, the two-qubit ensemble is left to decohere by the effect of natural relaxation, and no further control is applied. Constant coherence in a reference basis is then observed for timescales of the order of a second. Coherence is measured according to a variety of recently proposed quantifiers [21], and its permanence is found to be measure-independent. We also reveal how coherence quantitatively captures a dynamical interplay between classical and general quantum correlations [22], while any entanglement may rapidly disappear [23]. For more general initial states, we show how coherence can decay yet remains above a guaranteed threshold at any time. This demonstration significantly advances our understanding of the resilience of quantum effects against decoherence, and shows that a total immunity of coherence to environmental noise is not only possible in principle, but can spontaneously occur in a real physical system. Our results have potential implications for quantum sensing [5] and other scenarios relying on the robust exploitation of quantum coherence in many-body systems.

Quantum coherence manifests when a quantum system is in a superposition of multiple states taken from a reference basis. The reference basis is specified by the physics of the problem under investigation, for instance one may focus on the energy eigenbasis when addressing coherence in transport phenomena and thermodynamics. Here, for an N -qubit system, we will fix the reference basis to be the ‘plus/minus’ basis $\{|\pm\rangle^{\otimes N}\}$, where $\{|\pm\rangle\}$ are the eigenstates of the σ_1 Pauli operator, which describes the x component of the spin on each qubit [16]. Any state with density matrix δ diagonal in the plus/minus basis will be referred to as incoherent. According to a recently formulated resource theory [21, 24], the degree of quantum coherence in the state ρ of a quantum system can be quantified in terms of how distinguishable ρ is from the set of incoherent states,

$$C_D(\rho) = \inf_{\delta \text{ incoherent}} D(\rho, \delta), \quad (1)$$

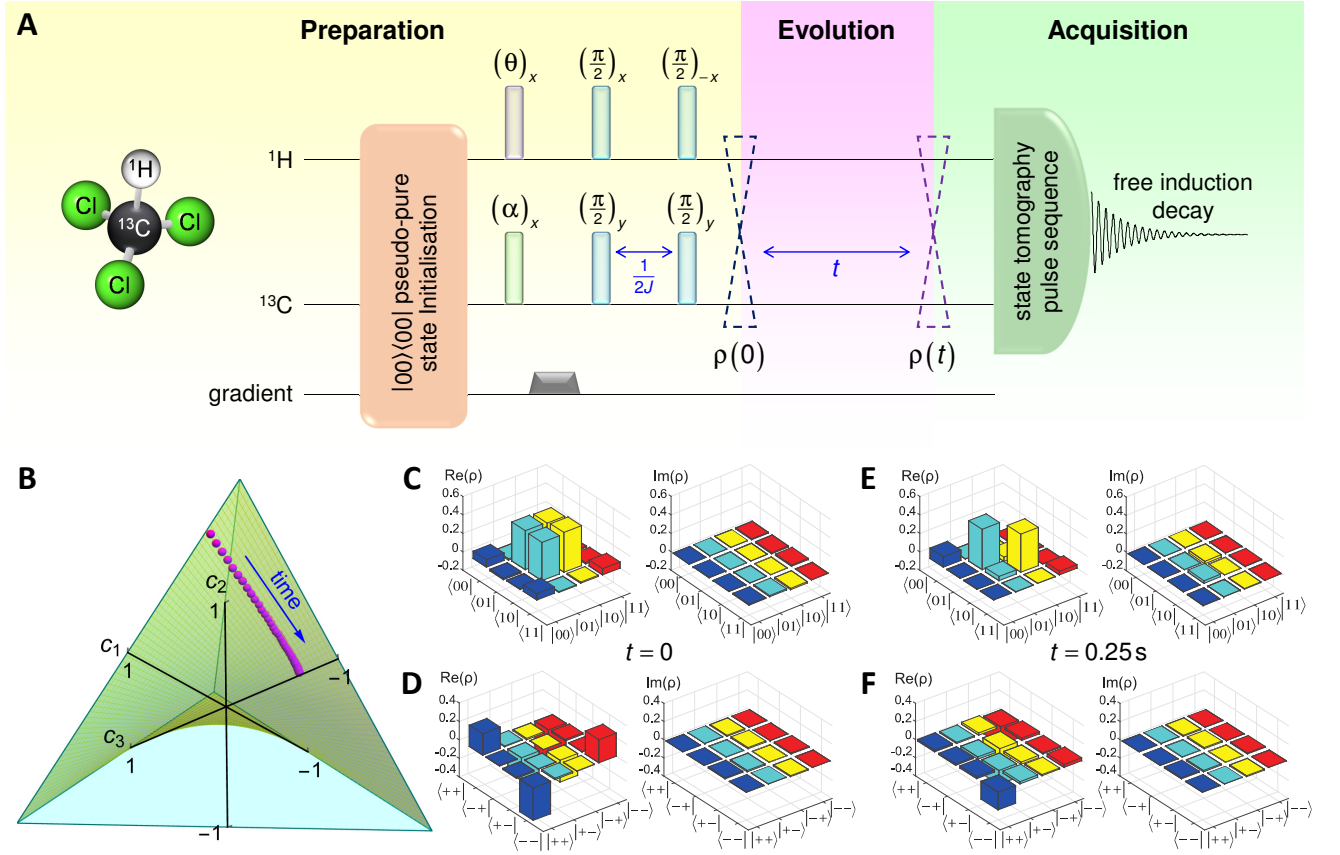


FIG. 1. **A:** Plan of the experiment with detail of the pulse sequence to prepare two-qubit BD states ρ encoded in the spins of the ^1H and ^{13}C nuclei of the Chloroform sample. **B:** Dynamical evolution of the experimental states $\rho(t)$ (magenta points) in the space of their spin-spin correlation triple $c_j = \langle \sigma_j \otimes \sigma_j \rangle$, $j = 1, 2, 3$; all BD states of Eq. (2) fill the light blue tetrahedron, while the subclass of states spanning the lime green surface inscribed within the tetrahedron are predicted to have time-invariant coherence in the plus/minus basis according to any valid measure defined as in Eq. (1). The remaining panels illustrate full tomographies of the experimental states as prepared at time $t = 0$ (**C, D**) and after $t = 0.25$ s of free evolution in a natural phase damping environment (**E, F**); the top row corresponds to the computational basis, and the bottom row to the plus/minus basis.

where the distance D is assumed jointly convex and contractive under quantum channels, as detailed in the Appendix. In general, different measures of coherence induce different orderings on the space of quantum states, as it happens for entanglement and other quantum resources. A consequence of this fact is that, for states of a single qubit, it is impossible to find a nontrivial noisy dynamics under which coherence is naturally preserved [17] when measured with respect to all possible choices of D in Eq. (1). As we report here, such a counterintuitive situation can occur instead for larger composite systems.

We encoded a two-qubit system in a Chloroform (CHCl_3) sample enriched with ^{13}C , where the ^1H and ^{13}C spin- $\frac{1}{2}$ nuclei are associated to the first and second qubit, respectively. This setup realises a highly effective quantum simulator, in which two-qubit states ρ can be prepared as pseudo-pure states [18, 19] by manipulating the deviation matrix from the thermal equilibrium density operator of the ensemble, via the application of radiofrequency (rf) pulses and evolution under spin interactions [16, 20]. The experiment was performed in a Varian 500 MHz liquid-NMR spectrometer at room temper-

ature, according to the plan illustrated in Fig. 1A. The state preparation stage allowed us to initialise the system in any state obtained as a mixture of maximally entangled Bell states, that is, any Bell diagonal (BD) state of two qubits [26]. These states take the form

$$\rho = \frac{1}{4} \left(\mathbb{I} \otimes \mathbb{I} + \sum_{j=1}^3 c_j \sigma_j \otimes \sigma_j \right), \quad (2)$$

where $\{\sigma_j\}$ are the Pauli matrices and \mathbb{I} is the identity operator on each qubit; they are completely specified by the spin-spin correlation functions $c_j = \langle \sigma_j \otimes \sigma_j \rangle$ for $j = 1, 2, 3$, and can be conveniently represented in the space spanned by these three parameters as depicted in Fig. 1B. We aimed to prepare specifically a BD state with initial correlation functions $c_1(0) = 1$, $c_2(0) = 0.7$ and $c_3(0) = -0.7$, by first initialising the system in the pseudo-pure state $|00\rangle\langle 00|$ as described in Refs. [16, 18], and then implementing the sequence of rf pulses shown in Fig. 1A with $\theta = \pi$ and $\alpha = \arccos(-0.7) \approx 134^\circ$.

After state preparation, the system was allowed to evolve freely during a period of time t , with t increased for each trial

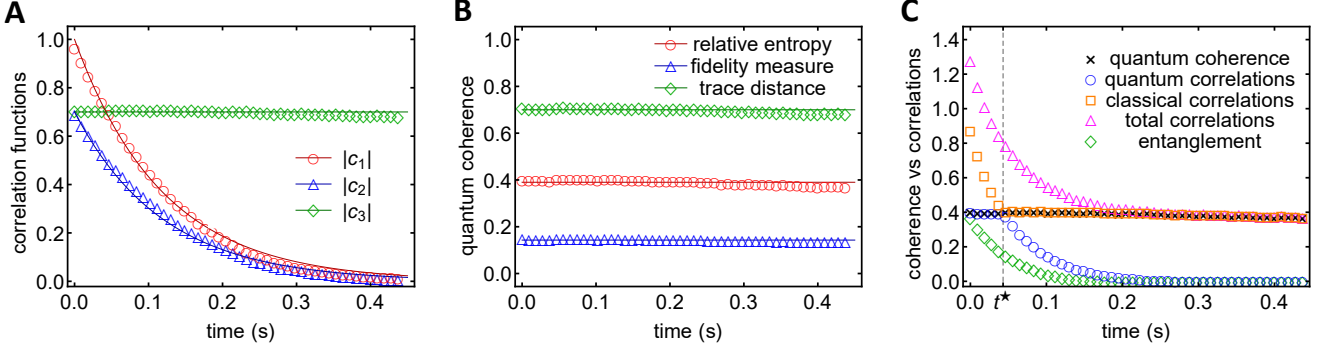


FIG. 2. **A:** Dynamics of the absolute values of the spin-spin correlation functions $|c_j| = |\langle \sigma_j \otimes \sigma_j \rangle|$, $j = 1, 2, 3$, in the prepared two-qubit state. The dots correspond to experimental data, as also visualised in Fig. 1B. The solid lines correspond to theoretical predictions based on phase damping noise with our measured characteristic relaxation times. **B:** Experimental demonstration of time-invariant quantum coherence (in the plus/minus basis) regardless of how measured. The red circles correspond to the relative entropy of coherence [21], the blue triangles to the fidelity-based geometric measure of coherence [24], the green diamonds to the (normalised) trace distance of coherence [17], which is equal to the l_1 norm of coherence [21] in our states; see Appendix for definitions. The slight negative slope is due to the subdominant effect of amplitude damping. **C:** Dynamics of coherence and all forms of correlations [25] in the prepared state, measured according to relative entropies. Coherence aligns with constant quantum correlations before the switch time, and with constant classical correlations after the switch time. The switch time t^* is in excellent agreement with the prediction based on our measured relaxation times, $t^* = \frac{T_1^H T_2^C}{T_1^H + T_2^C} \ln \left| \frac{c_1(0)}{c_3(0)} \right| \approx 0.043$ s. Theoretical curves are omitted for graphical clarity. In all panels, experimental errors due to small pulse imperfections (0.3% per pulse) result in error bars within the size of the data points.

in increments of $2/J$ from 0 to 0.5 s (where $J \approx 215$ Hz is the scalar spin-spin coupling constant, see Appendix), in order to obtain the complete relaxation process. In the employed setup, the two main sources of decoherence can be modelled as Markovian phase damping and generalised amplitude damping channels acting on each qubit, with characteristic relaxation times T_2 and T_1 , respectively (see Appendix). For our system, the relaxation times were measured as $T_1^H = 7.53$ s, $T_2^H = 0.14$ s, $T_1^C = 12.46$ s, $T_2^C = 0.90$ s which implies that $T_1^{H,C} \gg T_2^{H,C}$. Therefore, considering also the time domain of the experiment, only the phase damping noise can be assumed to have a dominant effect.

The final step consisted of performing full quantum state tomography for each interval of time t , following the procedure detailed in Appendix. Instances of the reconstructed experimental states at $t = 0$ and $t = 0.25$ s are presented in Fig. 1C–F. The fidelity of the initial state with the ideal target was measured at 99.1%, testifying the high degree of accuracy of our preparation stage. We verified that the evolved state remained of the BD form Eq. (2) during the whole relaxation with fidelities above 98.5%: we could then conveniently visualise the dynamics focusing on the evolution of the spin-spin correlation triple $\{c_j(t)\}$, as indicated by magenta points in Fig. 1B. The time evolution of the triple $\{c_j(t)\}$ is shown in detail in Fig. 2A.

From the acquired state tomographies during the relaxation progress, we measured the dynamics of quantum coherence in our states adopting all the *bona fide* coherence quantifiers proposed in recent literature, as shown in Fig. 2B. All measures were found simultaneously constant within the experimental confidence levels, revealing a universal resilience of quantum coherence in the dynamics under investigation. We remark

that the observed measure-independent time-invariant coherence is a highly nontrivial phenomenon which can only occur under peculiar dynamical conditions. A theoretical analysis (see Ref. [17] and Appendix) predicts in fact that, for all BD states evolving such that their spin-spin correlations obey the condition $c_2(t) = -c_1(t)c_3(t)$ (corresponding to the lime green surface in Fig. 1B), any valid measure of coherence as defined in Eq. (1) with respect to the plus/minus basis should remain constant at any time t . As evident from the placement of the data points in Fig. 1B, our setup realised precisely the predicted dynamical conditions for time-invariant coherence, with no further control during the relaxation. Our experiment thus demonstrated a natural occurrence of indestructible quantum coherence under Markovian decoherence for the first time.

It is important to note that the observed effect is distinct from an instance of decoherence-free subspace [27]. In the latter case, an open system dynamics can act effectively as a unitary evolution on a subset of quantum states, whose informational properties are therefore all automatically preserved. In our case, the states are instead degraded with time, but only their coherence in the considered reference basis remains unaffected. We verified this by measuring other indicators of correlations [25] in our states as a function of time. Fig. 2C shows the dynamics of entanglement, classical, quantum, and total correlations (defined in the Appendix), as well as coherence. While entanglement is found to undergo a sudden death [23, 28] at ≈ 0.21 s, a sharp transition between the decay of classical and quantum correlations is observed at the switch time $t^* \approx 0.043$ s. Such a puzzling feature has been reported before theoretically [22, 29] and experimentally [26, 30, 31], but here we unfold the prominent role played by coherence in

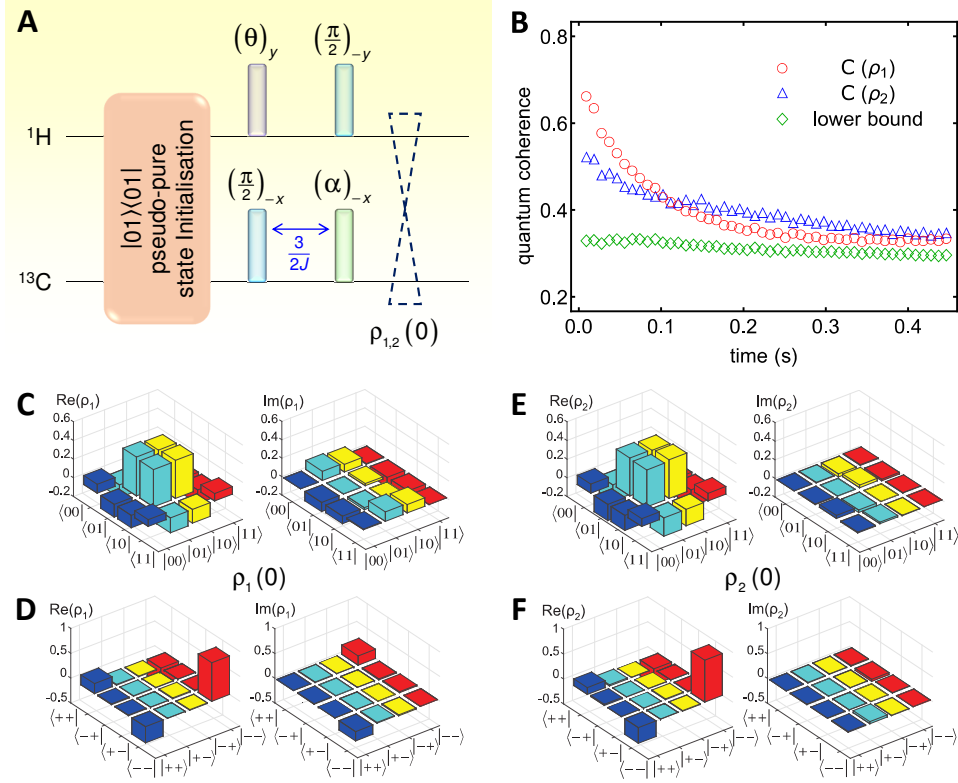


FIG. 3. **A**: Modified preparation stage to engineer two-qubit states not in the BD form. We prepared two pseudo-pure states ρ_1 and ρ_2 with purity 0.92 and 0.93 respectively, setting phases $\theta \approx 0.94$ rad, $\alpha = \pi/3$ for ρ_1 , and $\theta \approx 0.78$ rad, $\alpha = \pi/2$ for ρ_2 . The experiment then proceeded with the evolution and acquisition stages as in Fig. 1A. Tomographical reconstructions of the experimental states at time $t = 0$ are presented in panels **C** (ρ_1 , computational basis), **D** (ρ_1 , plus/minus basis), **E** (ρ_2 , computational basis), **F** (ρ_2 , plus/minus basis). Panel **B** shows the dynamics of the (relative entropy of) quantum coherence in the prepared states under spontaneous relaxation, as well as its lower bound inferred from the evolution of their spin-spin correlation functions.

this dynamical picture. Namely, coherence in the plus/minus basis is found quantitatively equal to quantum correlations before the switch time, and to classical ones after the switch time, henceforth remaining constant at all times. This novel interplay between coherence and correlations, demonstrated in our natural decohering conditions, manifests once again for any valid choice of geometric quantifiers used to measure the involved quantities [17]; as an instance, in Fig. 2C we picked all measures based on relative entropy.

One might now wonder how general the reported phenomena are if the initial states differ from the class of BD states of Eq. (2). In the Appendix we prove that, given an arbitrary two-qubit state ρ with spin-spin correlation functions $\{c_j\}$, its coherence with respect to any basis is always larger than the coherence of the BD state defined by the same correlation functions (this result in fact extends to quantum systems of any number of qubits). This entails that, even if coherence in arbitrary states may decay under decoherence, it will stay above a threshold guaranteed by the coherence of corresponding BD states. To demonstrate this, we modified the preparation stage of our experiment as illustrated in Fig. 3A, in order to engineer more general two-qubit states. We prepared two different pseudo-pure states ρ_1 and ρ_2 (see Fig. 3C–F), both with matching initial correlation triple $c_1(0) = 0.95$, $c_2(0) = 0.62$,

$c_3(0) = -0.65$, within the experimental accuracy. We then measured the dynamics of their coherence under natural relaxation as before. For both of them, we observed a decay of coherence (albeit with different rates) towards a common time-invariant lower bound, which yielded a protected degree of coherence even after complete relaxation. The lower bound was determined solely by the evolution of the spin-spin correlation functions, regardless of the specifics of the states.

In conclusion, we demonstrated in a room temperature NMR implementation that coherence, the quintessential signature of quantum mechanics, can perfectly resist decoherence under particular dynamical conditions with no need for external control. While only certain composite states feature exactly constant coherence in time, we showed that more general states still maintain a guaranteed amount of coherence even in extreme noise conditions. These phenomena are universal in the sense that they manifest regardless of how one quantifies coherence within the operative framework of Eq. (1), thus qualifying as physical defining traits of the concept of coherence itself, rather than mathematical accidents related to some specific measure. Moreover, they are predicted to occur in larger systems composed by an arbitrary number of qubits [17]. It is intriguing then to wonder whether biological systems such as light-harvesting

complexes, in which quantum coherence effects have been observed under exposure to dephasing environments [9–11], might have evolved towards exploiting natural noise-tolerant mechanisms for coherence protection similar to the ideal one reported here; this is a topic for further investigation [8].

Regarding practical applications, our findings impact on all quantum and nanoscale technologies which rely on coherence as a resource and unavoidably operate in noisy conditions: we showed that their performance can run in principle unperturbed, baffling some forms of decoherence. In particular, in quantum metrology [5], coherence in the plus/minus basis is a resource for precise estimation of frequencies or magnetic fields generated by a Hamiltonian aligned along the spin- x direction. When decoherence with a preferred transversal direction (e.g., phase damping noise) affects the estimation, as in typical implementations of atomic magnetometry [32, 33],

it has been recently shown that a quantum enhancement can be achieved by optimising the evolution time [33, 34] or using error correcting techniques [35, 36]. Here we uncovered a case in which coherence is totally unaffected by transversal dephasing noise. This suggests that the states prepared here, and their many-qubit counterparts [17], could be used as metrological probes with sensitivity automatically immune to decoherence. We will explore these applications in future work.

Acknowledgments. This work was supported by the European Research Council [ERC StG GQCOP Grant No. 637352], the Brazilian funding agencies FAPERJ, CNPq [PDE Grant No. 236749/2012-9], CAPES [Pesquisador Visitante Especial-Grant No. 108/2012], and the Brazilian National Institute of Science and Technology of Quantum Information (INCT/IQ).

-
- [1] J. P. Dowling and G. J. Milburn, *Philos. T. Roy. Soc. A* **361**, 1655 (2003).
 - [2] D. Delpy *et al.* (UK QT SAB), “National strategy for quantum technologies,” (2015), <https://www.epsrc.ac.uk/newsevents/pubs/quantumtechstrategy/>.
 - [3] A. J. Leggett, *Prog. Theor. Phys. Suppl.* **69**, 80 (1980).
 - [4] R. J. Glauber, *Phys. Rev.* **130**, 2529 (1963).
 - [5] V. Giovannetti, S. Lloyd, and L. Maccone, *Science* **306**, 1330 (2004).
 - [6] M. Lostaglio, D. Jennings, and T. Rudolph, *Nature Commun.* **6**, 6383 (2015).
 - [7] S. Gerlich, S. Eibenberger, M. Tomandl, S. Nimmrichter, K. Hornberger, P. J. Fagan, J. Tüxen, M. Mayor, and M. Arndt, *Nature Commun.* **2**, 263 (2011).
 - [8] S. Lloyd, *J. Phys.: Conf. Ser.* **302**, 012037 (2011).
 - [9] G. S. Engel, T. R. Calhoun, E. L. Read, T.-K. Ahn, T. Mančal, Y.-C. Cheng, R. E. Blakenship, and G. R. Fleming, *Nature* **446**, 782 (2007).
 - [10] G. Panitchayangkoon, D. Hayes, K. A. Fransted, J. R. Caram, E. Harel, J. Z. Wen, R. E. Blankenship, and G. S. Engel, *PNAS* **107**, 12766 (2010).
 - [11] A. W. Chin, R. Rosenbach, F. Caycedo-Soler, S. F. Huelga, and M. B. Plenio, *Nature Phys.* **9**, 113 (2013).
 - [12] W. H. Zurek, *Rev. Mod. Phys.* **75**, 715 (2003).
 - [13] L. Viola, E. Knill, and S. Lloyd, *Phys. Rev. Lett.* **82**, 2417 (1999).
 - [14] A. M. Souza, G. A. Álvarez, and D. Suter, *Phys. Rev. Lett.* **106**, 240501 (2011).
 - [15] H. Rabitz, R. de Vivie-Riedle, M. Motzkus, and K. Kompa, *Science* **288**, 824 (2000).
 - [16] M. Nielsen and I. Chuang, *Quantum Computation and Quantum Information* (Cambridge University Press, Cambridge, 2000).
 - [17] T. R. Bromley, M. Cianciaruso, and G. Adesso, *Phys. Rev. Lett.* **114**, 210401 (2015).
 - [18] E. Knill, I. Chuang, and R. Laflamme, *Phys. Rev. A* **57**, 3348 (1998).
 - [19] Y. Sharf, T. F. Havel, and D. G. Cory, *Phys. Rev. A* **62**, 052314 (2000).
 - [20] I. S. Oliveira, T. J. Bonagamba, R. S. Sarthour, J. C. C. Freitas, and E. R. de Azevedo, *NMR Quantum Information Processing* (Elsevier, Amsterdam, 2007).
 - [21] T. Baumgratz, M. Cramer, and M. B. Plenio, *Phys. Rev. Lett.* **113**, 140401 (2014).
 - [22] L. Mazzola, J. Piilo, and S. Maniscalco, *Phys. Rev. Lett.* **104**, 200401 (2010).
 - [23] T. Yu and J. H. Eberly, *Science* **323**, 598 (2009).
 - [24] A. Streltsov, U. Singh, H. S. Dhar, M. N. Bera, and G. Adesso, *Phys. Rev. Lett.* **115**, 020403 (2015).
 - [25] K. Modi, A. Brodutch, H. Cable, T. Paterek, and V. Vedral, *Rev. Mod. Phys.* **84**, 1655 (2012).
 - [26] F. M. Paula, I. A. Silva, J. D. Montealegre, A. M. Souza, E. R. de Azevedo, R. S. Sarthour, A. Saguia, I. S. Oliveira, D. O. Soares-Pinto, G. Adesso, and M. S. Sarandy, *Phys. Rev. Lett.* **111**, 250401 (2013).
 - [27] P. G. Kwiat, A. J. Berglund, J. B. Altepeter, and A. G. White, *Science* **290**, 498 (2000).
 - [28] M. P. Almeida, F. de Melo, M. Hor-Meyll, A. Salles, S. P. Walborn, P. H. S. Ribeiro, and L. Davidovich, *Science* **316**, 579 (2007).
 - [29] M. Cianciaruso, T. R. Bromley, W. Roga, R. Lo Franco, and G. Adesso, *Sci. Rep.* **5**, 10177 (2015).
 - [30] J.-S. Xu, X.-Y. Xu, C.-F. Li, C.-J. Zhang, X.-B. Zou, and G.-C. Guo, *Nature Commun.* **1**, 7 (2010).
 - [31] R. Auccaise, L. C. Céleri, D. O. Soares-Pinto, E. R. de Azevedo, J. Maziero, A. M. Souza, T. J. Bonagamba, R. S. Sarthour, I. S. Oliveira, and R. M. Serra, *Phys. Rev. Lett.* **107**, 140403 (2011).
 - [32] W. Wasilewski, K. Jensen, H. Krauter, J. J. Renema, M. V. Balabas, and E. S. Polzik, *Phys. Rev. Lett.* **104**, 133601 (2010).
 - [33] J. B. Brask, R. Chaves, and J. Kołodyński, *Phys. Rev. X* **5**, 031010 (2015).
 - [34] R. Chaves, J. B. Brask, M. Markiewicz, J. Kołodyński, and A. Acín, *Phys. Rev. Lett.* **111**, 120401 (2013).
 - [35] W. Dür, M. Skotiniotis, F. Fröwis, and B. Kraus, *Phys. Rev. Lett.* **112**, 080801 (2014).
 - [36] E. M. Kessler, I. Lovchinsky, A. O. Sushkov, and M. D. Lukin, *Phys. Rev. Lett.* **112**, 150802 (2014).
 - [37] G. L. Long, H. Y. Yan, and Y. Sun, *J. Opt. B: Quantum Semi-class. Opt.*, 376 (2001).
 - [38] F. G. S. L. Brandão and G. Gour, *Phys. Rev. Lett.* **115**, 070503 (2015).
 - [39] V. Vedral, M. B. Plenio, M. A. Rippin, and P. L. Knight, *Phys. Rev. Lett.* **78**, 2275 (1997).
 - [40] K. Modi, T. Paterek, W. Son, V. Vedral, and M. Williamson, *Phys. Rev. Lett.* **104**, 080501 (2010).
 - [41] T. R. Bromley, M. Cianciaruso, R. Lo Franco, and G. Adesso,

- J. Phys. A: Math. Theor. **47**, 405302 (2014).
- [42] F. M. Paula, A. Saguia, T. R. de Oliveira, and M. S. Sarandy, Europhys. Lett. **108**, 10003 (2014).
- [43] B. Aaronson, R. Lo Franco, G. Compagno, and G. Adesso, New J. Phys. **15**, 093022 (2013).
- [44] M. F. Cornelio, O. Jiménez Farías, F. F. Fanchini, I. Frerot, G. H. Aguilar, M. O. Hor-Meyll, M. C. de Oliveira, S. P. Walborn, A. O. Caldeira, and P. H. S. Ribeiro, Phys. Rev. Lett. **109**, 190402 (2012).
- [45] M. Cianciaruso, T. R. Bromley, and G. Adesso, arXiv:1507.01600 (2015), arXiv:arXiv:1507.01600.

Appendix A: Experimental details

1. NMR setup

The NMR experiments were performed encoding the desired two-qubit systems in a Chloroform (CHCl_3) sample enriched with ^{13}C , prepared as a mixture of 100 mg of 99% ^{13}C -labelled CHCl_3 in 0.7 mL of 99.8% CDCl_3 . The ^1H and ^{13}C spin-1/2 nuclei were associated to the first and second qubit, respectively. This system is described by the Hamiltonian

$$\mathcal{H} = \hbar\omega_H I_z^H + \hbar\omega_C I_z^C + 2\pi\hbar J I_z^H I_z^C, \quad (\text{A1})$$

where I_z^k is the z component of the spin angular momentum of each nucleus $k = H, C$, and ω_k is their Larmour frequency. On a Varian 500 MHz liquid-NMR spectrometer, where the experiments were implemented, it corresponds to $\omega_H/2\pi \approx 500\text{MHz}$ and $\omega_C/2\pi \approx 125\text{MHz}$, where J represents the weak scalar spin-spin coupling which was measured at $\approx 215\text{ Hz}$.

The experiments were performed at room temperature, so that the high temperature approximation ($k_B T \gg \hbar\omega_L$) guarantees that the thermal equilibrium density operator related to this Hamiltonian, $\rho_0 = e^{-\mathcal{H}/k_B T}/\mathcal{Z}$, can be simplified to

$$\rho_0 \approx \frac{1}{4} (\mathbb{I}^A \otimes \mathbb{I}^B + \epsilon \Delta\rho), \quad (\text{A2})$$

where $\mathcal{Z} = \sum_m e^{-E_m/k_B T}$ is the associated partition function, $\Delta\rho = I_z^H + 4I_z^C$ is the so-called deviation matrix, and $\epsilon = \hbar\omega_H/k_B T \sim 10^{-5}$. The application of radiofrequency (rf) pulses and the evolution under spin interactions allow for easy manipulation of the thermal state ρ_0 in order to produce different states with an excellent control of angle and phase. This procedure is described by the Hamiltonian

$$\mathcal{H} = \hbar(\omega_H - \omega_{rf}^H) I_z^H + \hbar(\omega_C - \omega_{rf}^C) I_z^C - \hbar\omega_1^H (I_x^H \cos\phi^H + I_y^H \sin\phi^H) - \hbar\omega_1^C (I_x^C \cos\phi^C + I_y^C \sin\phi^C) \quad (\text{A3})$$

where ω_{rf}^k is the frequency of the rf field for nucleus k (on resonance: $\omega_{rf}^k \approx \omega_k$), ω_1^k is the nutation angle and ϕ^k their respective phase. As only the deviation matrix $\Delta\rho$ is affected by those unitary transformations, it is convenient to write the resulting state as $\rho_{\text{total}} = [(1 - \epsilon)(\mathbb{I}^A \otimes \mathbb{I}^B) + \epsilon\rho]/4$, from which we define the logical NMR density matrix as the state $\rho \equiv [(\mathbb{I}^A \otimes \mathbb{I}^B) + \Delta\rho]/4$. The state preparation procedure discussed in the main text refers to engineering ρ into any desired two-qubit state.

2. Decoherence processes

NMR naturally provides well characterised environments, characterised by the Phase Damping (PD) and Generalised Amplitude Damping (GAD) channels acting on each qubit [16]. PD is associated to loss of coherence (in the computational basis) with no energy exchange and is specified by the following Kraus operators,

$$K_0^P = \sqrt{1 - \frac{q(t)}{2}} \mathbb{I}, \quad K_3^P = \sqrt{\frac{q(t)}{2}} \sigma_3, \quad (\text{A4})$$

where the $q(t)$ damping function is related to the characteristic relaxation time T_2 by $q(t) = (1 - e^{-t/T_2})$.

On the other hand, the GAD channel is associated to energy exchange between system and environment and can be written in Kraus operator form by

$$K_0^G = \sqrt{p} \begin{pmatrix} 1 & 0 \\ 0 & \sqrt{1-u(t)} \end{pmatrix}, \quad K_1^G = \sqrt{p} \begin{pmatrix} 0 & \sqrt{u(t)} \\ 0 & 0 \end{pmatrix}, \\ K_2^G = \sqrt{1-p} \begin{pmatrix} \sqrt{1-u(t)} & 0 \\ 0 & 1 \end{pmatrix}, \quad K_3^G = \sqrt{1-p} \begin{pmatrix} 0 & 0 \\ \sqrt{u(t)} & 0 \end{pmatrix}, \quad (\text{A5})$$

where $u(t) = 1 - e^{-t/T_1}$ and $p = 1/2 - \alpha$ with $\alpha = \hbar\omega_L/2k_B T$.

As shown in Fig. 1A of the main text, during the evolution period no refocusing pulses were applied. This implies that the phase damping function $q(t)$ decayed naturally according to the characteristic relaxation time T_2 . We note that the effective T_2 for our experiment depends not only on the thermally induced fluctuations of longitudinal fields (standard NMR T_2 contribution) but also on static field inhomogeneities. This dependence makes the PD decoherence process occur faster, guaranteeing that no GAD effects should be effectively observed during the experiment time domain. The characteristic relaxation times were measured as $T_1^H = 7.53\text{ s}$, $T_2^H = 0.14\text{ s}$, $T_1^C = 12.46\text{ s}$, $T_2^C = 0.90\text{ s}$, which satisfy $T_1 \gg T_2$, as desired.

3. Quantum state tomography

The quantum state tomography was performed applying the simplified procedure proposed in Ref. [37]. In this case the full matrix reconstruction is obtained after performing the local operations: II, IX, IY, XX on each qubit. Here, I, X and Y , correspond, respectively, to the identity operation, a $\pi/2$ rotation around the x -axis, and a $\pi/2$ rotation around the y -axis. This set of operations provides a 16×16 system of equations, whose solution gives the density matrix elements.

Appendix B: Theoretical details

1. Geometric approach to quantifying coherence and correlations

A rigorous and general formalism to quantify the coherence of a d -dimensional quantum state ρ with respect to a given

reference basis $\{|e_i\rangle\}_{i=1}^d$ can be found in [21] within the setting of quantum resource theories [38]. Natural candidates for quantifying coherence arise from a rather intuitive geometric approach, wherein the distance from ρ to the set of states diagonal in the reference basis (known as incoherent states) is considered, provided the adopted distance satisfies the following constraints: contractivity under completely positive trace preserving (CPTP) maps, i.e. $D(\Phi(\rho), \Phi(\tau)) \leq D(\rho, \tau)$ for any CPTP map Φ ; joint convexity, i.e. $D(\sum_i p_i \rho_i, \sum_i p_i \tau_i) \leq \sum_i p_i D(\rho_i, \tau_i)$ for any probability distribution $\{p_i\}$; plus some additional properties listed in [39]. In particular,

$$C_D(\rho) \equiv \inf_{\delta \in \mathcal{I}} D(\rho, \delta), \quad (\text{B1})$$

with \mathcal{I} being the set of incoherent states, defines full coherence monotones C_D if one chooses for example the following distance functionals: relative entropy distance [21] $D_{RE}(\rho, \tau) = S(\rho||\tau)$, where $S(\rho||\tau) = \text{Tr}[\rho(\log(\rho) - \log(\tau))]$ is the quantum relative entropy; and fidelity based distance [24] $D_F(\rho, \tau) = 1 - F(\rho, \tau)$, where $F(\rho, \tau) = \left(\text{Tr}\left(\sqrt{\sqrt{\rho}\tau\sqrt{\rho}}\right)\right)^2$ is the Uhlmann fidelity. It is still currently unknown whether the trace distance $D_{\text{Tr}}(\rho, \tau) = \text{Tr}\left(\sqrt{(\rho - \tau)^2}\right)$ induces a valid measure of coherence, even though it is both contractive and jointly convex (note we adopt a normalised definition equal to twice the conventional trace distance). However, for BD states the trace distance of coherence is equal to the l_1 norm of coherence, which is a full coherence monotone [17, 21].

Analogously, one can define faithful measures of correlations such as total correlations, discord-type quantum correlations and entanglement in the following way: for total correlations,

$$T_D(\rho) \equiv \inf_{\pi \in \mathcal{P}} D(\rho, \pi), \quad (\text{B2})$$

where $\pi = \rho^A \otimes \tau^B$, with ρ^A (τ^B) being an arbitrary state of subsystem A (B), form the set of product states \mathcal{P} ; for quantum correlations [25],

$$Q_D(\rho) \equiv \inf_{\chi \in \mathcal{C}} D(\rho, \chi), \quad (\text{B3})$$

where $\chi = \sum_{ij} p_{ij} |i^A\rangle\langle i^A| \otimes |j^B\rangle\langle j^B|$, with $\{p_{ij}\}$ being a joint probability distribution and $\{|i^A\rangle\}$ ($\{|j^B\rangle\}$) an orthonormal basis of subsystem A (B), form the set of classical states \mathcal{C} ; for entanglement [39],

$$E_D(\rho) \equiv \inf_{\sigma \in \mathcal{S}} D(\rho, \sigma), \quad (\text{B4})$$

where $\sigma = \sum_i p_i \rho_i^A \otimes \tau_i^B$, with $\{p_i\}$ being a probability distribution and ρ_i^A (τ_i^B) arbitrary states of subsystem A (B), form the set of separable states \mathcal{S} .

Finally, within this unifying distance-based approach, yet in a quite different way, it is also possible to identify the classical correlations of a state ρ as follows:

$$P_D(\rho) \equiv \inf_{\chi_\rho} \inf_{\pi \in \mathcal{P}} D(\chi_\rho, \pi), \quad (\text{B5})$$

i.e. as the minimal distance between any closest classical state χ_ρ to ρ , and the set of product states [40–42].

2. Conditions for time-invariant coherence

We now outline the general conditions such that constant coherence can be observed for all time [17], constant quantum correlations can be observed up to a switch time t^* [29], and constant classical correlations can be observed after the switch time t^* , when considering two-qubit BD states undergoing local nondissipative decoherence.

Consider two qubits A and B initially in a BD state:

$$\rho(0) = \frac{1}{4} \left(\mathbb{I}^A \otimes \mathbb{I}^B + \sum_{\alpha=1}^3 c_\alpha(0) \sigma_\alpha^A \otimes \sigma_\alpha^B \right) \quad (\text{B6})$$

and such that the following special initial condition is satisfied,

$$c_i(0) = -c_j(0)c_k(0), \quad (\text{B7})$$

where \mathbb{I} is the 2×2 identity, σ_α is the α -th Pauli matrix and $\{i, j, k\}$ is a fixed chosen permutation of $\{1, 2, 3\}$. Let the two (noninteracting) qubits undergo local Markovian flip-type decoherence channels towards the k -th spin direction (i.e. bit-flip noise for $k = 1$, bit-phase-flip noise for $k = 2$, and phase-flip noise for $k = 3$). Their evolved global state at any time t is then represented by

$$\rho(t) = \sum_{\alpha, \beta=0}^3 K_\alpha \otimes K_\beta \rho(0) K_\alpha^\dagger \otimes K_\beta^\dagger, \quad (\text{B8})$$

where

$$K_0 = \sqrt{1 - \frac{q(t)}{2}} \mathbb{I}, \quad K_i = 0, \quad K_j = 0, \quad K_k = \sqrt{\frac{q(t)}{2}} \sigma_k, \quad (\text{B9})$$

$q(t) = 1 - e^{-\gamma t}$ is the strength of the noise, γ is the decoherence rate, and $\{i, j, k\}$ is the permutation of $\{1, 2, 3\}$ fixed in the initial condition, Eq. (B7). One can easily see that the evolved state is still a BD state, whose corresponding correlation function triple is given by

$$c_i(t) = c_i(0)e^{-2\gamma t}, \quad c_j(t) = c_j(0)e^{-2\gamma t}, \quad c_k(t) = c_k(0). \quad (\text{B10})$$

Focusing first on coherence, in [17] it was shown that, according to any contractive and jointly convex distance, one of the closest incoherent states $\delta_{\rho(t)}^{(a)}$ to the evolved BD state $\rho(t)$, with respect to the basis consisting of tensor products of eigenstates of σ_α , is just the Euclidean projection of $\rho(t)$ onto the c_α -axis, i.e. it is still a BD state and its triple is given by $\{\delta_{\alpha\beta} c_\alpha(t)\}_{\beta=1}^3$, for any $\alpha \neq i$. Moreover, in [41] it was shown that any contractive distance between the evolved BD state $\rho(t)$ and its Euclidean projection onto the c_j -axis must be constant for any t . It immediately follows that any valid distance-based measure of coherence $C_D^{(j)}(\rho(t))$ of the evolved state, with respect to the product basis consisting of tensor products of eigenstates of σ_j , is invariant for any time t .

For quantum correlations, according to any contractive and jointly convex distance, one of the closest classical states $\chi_{\rho(t)}$ to the evolved BD state $\rho(t)$ is just the Euclidean projection of $\rho(t)$ onto the closest c -axis, with triple given by $\{\delta_{\alpha\beta} c_\alpha(t)\}_{\beta=1}^3$

and α set by $|c_\alpha(t)| = \max\{|c_\beta(t)|\}_{\beta=1}^3$. When $|c_j(0)| > |c_k(0)|$ then $\alpha = j$ until the switch time $t^* = \frac{1}{2\gamma} \ln \left| \frac{c_j(0)}{c_k(0)} \right|$, with $\alpha = k$ afterwards. Combined with the result in [41] that any contractive distance between the evolved BD state $\rho(t)$ and its Euclidean projection onto the c_j -axis must be constant for any t , this immediately implies time-invariance of quantum correlations up until the switch time t^* . No general proof has yet been found for the subsequent time-invariance of classical correlations after the switch time t^* for any contractive and jointly convex distance, but this has been observed in particular cases (based e.g. on relative entropy, trace and fidelity based distances) [22, 41, 43]. The time-invariance of classical correlations is related to the finite-time emergence of the pointer basis during the dynamics [26, 44].

We note that in our experiment we have implemented exactly an instance of the above conditions, specifically in the case $i = 2$, $j = 1$ and $k = 3$; the corresponding phase-flip noise reduces precisely to the PD channel occurring in NMR, as it can be seen by comparing the Kraus operators in Eqs. (A4) and (B8). The decoherence rate in our demonstration was given by $\gamma = \frac{T_2^H + T_2^C}{2T_2^H T_2^C}$. With this evolution, the switch time is obtained as $t^* = \frac{1}{2\gamma} \ln \left| \frac{c_1(0)}{c_3(0)} \right|$. For an initial BD state with $c_1(0) = 1$, $c_2(0) = 0.7$, $c_3(0) = -0.7$ as we prepared, respecting the constraint in Eq. (B7), the expected switch time was $t^* \approx 0.043$ s, which was found in excellent agreement with the experimental data. Time-invariant coherence in the plus/minus basis (i.e. the eigenbasis of σ_1) was observed according to any known valid geometric measure C_D (Fig. 2 of the main text). Entanglement and total correlations instead decay monotonically without experiencing any interval of time-invariance in the considered dynamical conditions.

3. Coherence lower bound from BD states

BD states are particular instances of a more general class of N -qubit states having all maximally mixed marginals and characterised only by the three correlations functions $c_j = \langle \sigma_j^{\otimes N} \rangle$, with $j = 1, 2, 3$, the so-called \mathcal{M}_N^3 states [17]:

$$\varpi = \frac{1}{2^N} \left(\mathbb{I}^{\otimes N} + \sum_{j=1}^3 c_j \sigma_j^{\otimes N} \right). \quad (\text{B11})$$

We now prove that the coherence of an arbitrary N -qubit state ρ , with correlation functions $c_j = \langle \sigma_j^{\otimes N} \rangle$, is lower bounded by the coherence of the \mathcal{M}_N^3 state defined by the same correlation functions. This holds regardless of the number of qubits N and when considering the basis consisting of tensor products of eigenstates of σ_j , for any $j = 1, 2, 3$ (e.g. the plus/minus basis when $j = 1$). Such a proof just relies on the following two results.

First, as shown in [45], any N -qubit state ρ can be transformed into an \mathcal{M}_N^3 state with the same correlation functions $c_j = \langle \sigma_j^{\otimes N} \rangle$ through the map Θ defined as follows:

$$\Theta(\rho) = \frac{1}{2^{2(N-1)}} \sum_{j=1}^{2^{2(N-1)}} U'_j \rho U_j'^{\dagger} \quad (\text{B12})$$

where U'_j are the following single-qubit local unitaries

$$\{U'_j\}_{j=1}^{2^{2(N-1)}} = \left\{ \mathbb{I}^{\otimes N}, \{U_{j_1}\}_{j_1=1}^{2^{2(N-1)}}, \{U_{j_2} U_{j_1}\}_{j_2 > j_1=1}^{2^{2(N-1)}}, \dots \right. \\ \left. \dots \{U_{j_{2(N-1)}} \dots U_{j_2} U_{j_1}\}_{j_2 > j_1=1}^{2^{2(N-1)}} \right\}, \quad (\text{B13})$$

with

$$\{U_j\}_{j=1}^{2^{2(N-1)}} = \left\{ (\sigma_1 \otimes \sigma_1 \otimes I^{\otimes N-2}), (I \otimes \sigma_1 \otimes \sigma_1 \otimes I^{\otimes N-3}), \dots, \right. \\ (I^{\otimes N-3} \otimes \sigma_1 \otimes \sigma_1 \otimes I), (I^{\otimes N-2} \otimes \sigma_1 \otimes \sigma_1), \\ (\sigma_2 \otimes \sigma_2 \otimes I^{\otimes N-2}), (I \otimes \sigma_2 \otimes \sigma_2 \otimes I^{\otimes N-3}), \dots, \\ \left. (I^{\otimes N-3} \otimes \sigma_2 \otimes \sigma_2 \otimes I), (I^{\otimes N-2} \otimes \sigma_2 \otimes \sigma_2) \right\}. \quad (\text{B14})$$

Second, as shown below, the map Θ is an incoherent operation with respect to the basis consisting of tensor products of eigenstates of σ_j , for any $j = 1, 2, 3$. An incoherent operation is a CPTP map that cannot create coherence, i.e. with Kraus operators $\{K_i\}$ satisfying $K_i \mathcal{I} K_i^\dagger \subset \mathcal{I}$ for all i , with \mathcal{I} the set of incoherent states with respect to the chosen reference basis. Since any coherence monotone must be non-increasing under incoherent operations [21], it follows that the coherence of $\Theta(\rho)$ is less than or equal to the corresponding coherence of ρ .

In what follows we will prove that Θ is an incoherent operation with respect to the basis consisting of tensor products of eigenstates of σ_1 (i.e. the plus/minus basis), although analogous proofs hold when considering the other two Pauli operators. Since the Kraus operators of the map Θ are given by $K_j = \frac{1}{2^{N-1}} U'_j$, in order for Θ to be an incoherent operation in the plus/minus basis we need that $U'_j \delta U_j'^{\dagger} \in \mathcal{I}$ for any $\delta \in \mathcal{I}$ and any $j \in \{1, \dots, 2^{2(N-1)}\}$, where \mathcal{I} is the set of states diagonal in this basis. This obviously holds for $j = 1$, being U'_1 the identity. On the other hand, as it can be seen from Eq. (B13), all the other single-qubit unitaries U'_j are just products of the single-qubit unitaries U_j listed in Eq. (B14), so that we just need to prove that $U_j \delta U_j^\dagger \in \mathcal{I}$ for any $\delta \in \mathcal{I}$ and for any $j \in \{1, \dots, 2(N-1)\}$. For any $j \in \{1, \dots, N-1\}$, U_j just leaves any state which is diagonal in the plus/minus basis invariant, it being a tensor product between two σ_1 's acting on two neighbouring qubits and the identity acting on the remaining ones. Otherwise, for any $j \in \{N, \dots, 2(N-1)\}$, U_j is the tensor product between two σ_2 's acting on two neighbouring qubits and the identity on the rest of the qubits. Consequently, by using $\sigma_2|\pm\rangle\langle\pm| = |\mp\rangle\langle\mp|$ and the fact that the general form of a state δ diagonal in the plus/minus basis is $\delta = \sum_{j_1, j_2, \dots, j_N = \pm} p_{j_1, j_2, \dots, j_N} |j_1, j_2, \dots, j_N\rangle\langle j_1, j_2, \dots, j_N|$, we have that, when e.g. $j = N$, then $U_N \delta U_N^\dagger = \sum_{j_1, j_2, \dots, j_N = \pm} p_{j_1, j_2, \dots, j_N} U_N |j_1, j_2, \dots, j_N\rangle\langle j_1, j_2, \dots, j_N| U_N^\dagger = \sum_{j_1, j_2, \dots, j_N = \pm} p_{j_1, j_2, \dots, j_N} |\pi(j_1), \pi(j_2), \dots, \pi(j_N)\rangle\langle \pi(j_1), \pi(j_2), \dots, \pi(j_N)|$, where $\pi(\pm) \equiv \mp$, so that $U_N \delta U_N^\dagger \in \mathcal{I}$. Analogously, one can see that all the remaining single-qubit local unitaries U_j are such that $U_j \delta U_j \in \mathcal{I}$, thus completing the proof.